



Research paper

Refined energy method for the elastic flexural-torsional buckling of steel H-section beam-columns Part II: Comparison and verification for elements LTU and LTR

Marian Giżejowski¹, Anna Barszcz², Paweł Wiedro³

Abstract: In investigations constituting Part I of this paper, the effect of approximations in the flexural-torsional buckling analysis of beam-columns was studied. The starting point was the formulation of displacement field relationships built straightforward in the deflected configuration. It was shown that the second-order rotation matrix obtained with keeping the trigonometric functions of the mean twist rotation was sufficiently accurate for the flexural-torsional stability analysis. Furthermore, Part I was devoted to the formulation of a general energy equation for FTB being expressed in terms of prebuckling stress resultants and in-plane deflections through the factor k_1 . The energy equation developed there was presented in several variants dependent upon simplified assumptions one may adopt for the buckling analysis, i.e. the classical form of linear eigenproblem analysis (LEA), the form of quadratic eigenproblem analysis (QEA) and refined (non-classical) forms of nonlinear eigenproblem analysis (NEA), all of them used for solving the flexural-torsional buckling problems of elastic beam-columns. The accuracy of obtained analytical solutions based on different approximations in the elastic flexural-torsional stability analysis of thin-walled beam-columns is examined and discussed in reference to those of earlier studies. The comparison is made for closed form solutions obtained in a companion paper, with a scatter of results evaluated for $k_1 = 1$ in the solutions of LEA and QEA, as well as for all the options corresponding to NEA. The most reliable analytical solution is recommended for further investigations. The solutions for selected asymmetric loading cases of the left support moment and the half-length uniformly distributed span load of a slender unrestrained beam-column are discussed in detail in Part II. Moreover, the paper constituting Part II investigates how the buckling criterion obtained for the beam-column laterally and torsionally unrestrained between the end sections might be applied for the member with discrete restraints. The recommended analytical solutions are verified with use of numerical finite element method results, considering beam-columns with a mid-section restraint. A variant of the analytical form of solutions recommended in these investigations may be used in practical application in the Eurocode's General Method of modern design procedures for steelwork.

¹Prof., DSc., PhD., Eng., Warsaw University of Technology, Faculty of Civil Engineering, Al. Armii Ludowej 16, 00-637 Warsaw, Poland, e-mail: marian.gizejowski@pw.edu.pl, ORCID: 0000-0003-0317-1764

²DSc, PhD., Eng., Warsaw University of Technology, Faculty of Civil Engineering, Al. Armii Ludowej 16, 00-637 Warsaw, Poland, e-mail: anna.barszcz@pw.edu.pl, ORCID: 0000-0002-6476-227X

³Msc., Eng., PhD Study, Warsaw University of Technology, Faculty of Civil Engineering, Al. Armii Ludowej 16, 00-637 Warsaw, Poland, e-mail: pawel.wiedro@pw.edu.pl, ORCID: 0000-0002-0410-7353

Keywords: steel beam-column, bisymmetric double-tee section, elastic behaviour, flexural-torsional buckling, numerical simulations, verification of analytical solutions

1. Introduction

The closed form solutions obtained in a companion paper [7] are dealt with in this paper. The solutions obtained there may be directly used for single span bisymmetric I and H shaped beam-columns being laterally and torsionally unrestrained (LTU) between supports, the boundary conditions of which are simply supported with end sections free to warp. Flexural-torsional buckling (FTB) of beam-columns with discrete lateral-torsional restraint (LTR) is affected by a continuity of lateral displacements and twist rotation, and their derivatives of minor axis rotation and twist over the lateral-torsional (LT) restraints. For an estimation of the critical state of beam-columns with discrete LT restraints, a simple approximate solution for the so-called critical segment may be adopted, cf. Salvadori [13, 15, 16]. Such a solution requires to consider the critical state of segments being spanned between the support and the neighbouring LT restraint or between two neighbouring LT restraints, assuming a discontinuity of the beam-column segments with regard to the out-of-plane postbuckling deformation state components and their derivatives. Then, the stability curve $M_{y,\max} - N$ created for the critical segment of the lowest critical load multiplier is a lower bound envelope of the curves predicted for all the other segments. The estimation method based on this approximation is named the Salvadori's method. This method is adopted hereafter for LTR cases, together with the NEA Option 1a presented in [7].

2. Comparison and verification of analytical solutions for LTU beam-columns

2.1. Beam-columns of symmetric bending moment distribution

In this subchapter, the solution of present study according to the Option 1a in the companion paper [7] is compared with that of a non-classical form developed by Mohri et al. [12]. One may notice that the non-classical solution to be compared with is valid only for symmetric bending moment diagrams. The general solution presented in [12] is expressed as follows:

$$(2.1) \quad M_{y,\max} = C_1 N_z \left[C_{2ZF} \pm \sqrt{(C_{2ZF})^2 + \frac{i_0^2 N_T}{N_z}} \right] \sqrt{\left(1 - \frac{N}{N_y}\right) \left(1 - \frac{N}{N_z}\right) \left(1 - \frac{N}{N_T}\right)}$$

where: $C_1 = \frac{\bar{C}_1}{\sqrt{k_1}}$, $C_2 = \frac{\bar{C}_2}{\sqrt{k_1}} \sqrt{\left(1 - \frac{N}{N_y}\right) \left(1 - \frac{N}{N_z}\right) / \left(1 - \frac{N}{N_T}\right)}$ and other notation as explained in the companion paper [7].

The constant \bar{C}_1 is dependent upon the moment distribution along the member length while \bar{C}_2 is associated with off-shear centre line load application and dependent upon the load distribution along the member length (the values of constant \bar{C}_1 and \bar{C}_2 given in the numerators of C_1 and C_2 , respectively, are those from Table 1 of Mohri et al. [12]).

Eq. (2.1) is equivalent to the following:

$$\left(\sqrt{\frac{k_1}{\zeta}} \frac{1}{\bar{C}_1} \frac{M_{y,\max}}{M_{cr,0}} \right)^2 = \left(1 - \frac{N}{N_y} \right) \left(1 - \frac{N}{N_z} \right) \left(1 - \frac{N}{N_T} \right)$$

$$\zeta = 1 + \frac{2M_{y,\max}\bar{C}_2 z_F}{\bar{C}_1 i_0^2 N_T \left(1 - \frac{N}{N_T} \right)}$$

The relationships between the coefficients of Option 1a of the present study and those of Mohri et al. [12] holding for the symmetric loading pattern yield:

$$\frac{1}{C_{bc}} = \sqrt{\frac{k_1}{\zeta}} \frac{1}{\bar{C}_1}$$

$$\frac{1}{\bar{C}_1} \rightarrow \frac{1}{C_{bs,\text{rem}}}$$

$$\frac{2M_{y,\max}\bar{C}_2}{\bar{C}_1} \rightarrow C_{bF}$$

One can notice that $C_{bs,\text{rem}}$ of present study corresponds to the coefficient \bar{C}_1 developed by Mohri et al. in [12] while C_{bF} corresponds to $\frac{2M_{y,\max}\bar{C}_2}{\bar{C}_1}$ calculated from the data given by Mohri et al. [12]. The conclusion is that the conversion factors $C_{bs,\text{rem}}$ and C_{bF} of present study can be directly related to those obtained in [12] for cases of the symmetric loading, and they are the same as those predicted for beams in [2, 3]. The final conclusion is that for equal and opposite end moments ($\psi_M = 1$) and no span loads, as well as for span shear centre loads (for $\psi_q = \psi_Q = 1$) with no end moments, solutions based on the Option 1a of this study, for any symmetric loading case, are the same as those predicted in studies of Mohri et al. [12]. Since the analytical model presented in [12] was verified by numerical finite element simulations based on the model built in ABAQUS software, showing a sufficient accuracy of the analytical model developed there, the same accuracy is kept for the solution developed in the present study.

2.2. Beam-columns of asymmetric bending moment distributions

Firstly, the comparison is made for the equivalent uniform moment factors of two load cases of the left end moment (Fig. 1) and half-length uniformly distributed load placed at the section shear centre (Fig. 2).

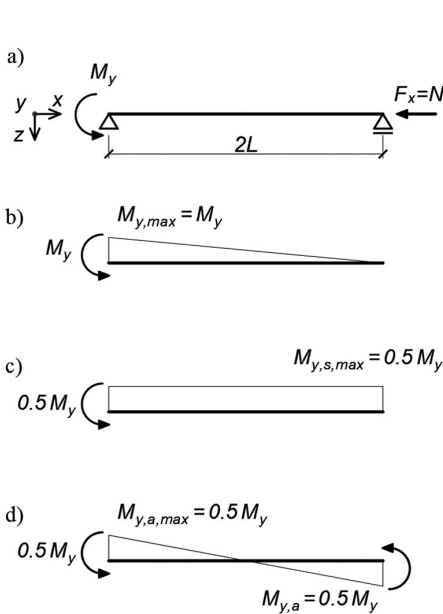


Fig. 1. Unrestrained beam-column with left end moment; a) static scheme, b) total moment diagram, c) symmetric moment component, d) antisymmetric moment component

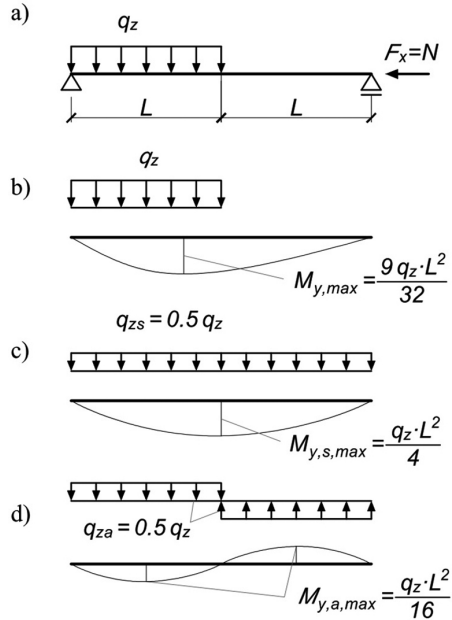


Fig. 2. Unrestrained beam-column with half-length uniformly distributed load; a) static scheme, b) total moment diagram, c) symmetric moment component, d) antisymmetric moment component

The equivalent uniform moment factors do not depend upon the beam-column length but for NEA based solutions depend upon the section property factor k_1 . The structure of equivalent uniform moment factor depends upon the assumptions used for M_y and M_z as explained in a companion paper [7]. Table 1 summarizes the NEA solutions based on the non-classical energy formulation presented there. The solutions based on LEA and QEA are summarized in Table 2.

Table 1. Comparison of the equivalent uniform moment factors for the non-classical energy formulation in which the minor axis moment of the energy equation is that of the second order

Type of NEA	Moment		Equivalent uniform moment factor C_{bc}
	M_y	M_z	
$M_z = M_z^{II}$	Option 1a	$M_y^{II,amp}$ $M_z^{II,amp}$	$\sqrt{\frac{\zeta}{k_1}} \left[\left(\frac{M_{y,s,max}}{M_{y,max}} \frac{1}{C_{bs,rem}} \right)^2 + \frac{\left(1 - \frac{N}{N_y}\right) \left(1 - \frac{N}{N_z}\right)}{\left(1 - \frac{N}{N_{ya}}\right) \left(1 - \frac{N}{N_{za}}\right)} \left(\frac{M_{y,a,max}}{M_{y,max}} \frac{1}{C_{ba,rem}} \right)^2 \right]^{-0.5}$

Continued on next page

Table 1 – Continued from previous page

Type of NEA	Moment		Equivalent uniform moment factor C_{bc}
	M_y	M_z	
$M_z = M_z^I$	Option 1b	$M_{y,P-\delta}^I$ $M_{z,amp}^I$	$\sqrt{\frac{\zeta}{k_1}} \left\{ \left(\frac{M_{y,s,max}}{M_{y,max}} \right)^2 \left[\left(1 - \frac{N}{N_y} \right) \left(\frac{1}{C_{bs,rem}} \right)^2 + \frac{N}{N_y} \frac{\pi^2 c \delta s}{C_{bs,rem1}} \right] + \frac{1 - \frac{N}{N_z}}{1 - \frac{N}{N_{za}}} \left(\frac{M_{y,a,max}}{M_{y,max}} \right)^2 \left[\left(1 - \frac{N}{N_y} \right) \left(\frac{1}{C_{ba,rem}} \right)^2 + \frac{1 - \frac{N}{N_y}}{1 - \frac{N}{N_{ya}}} \frac{N}{N_{ya}} \pi^2 c \delta a \frac{1}{C_{ba,rem1}} \right] \right\}^{-0.5}$
	Option 2	$M_{y,P-\delta}^I$ $M_{z,P-\delta}^I$	$\sqrt{\frac{\zeta}{k_1}} \left\{ \left(\frac{M_{y,s,max}}{M_{y,max}} \right)^2 \left[\left(1 - \frac{N}{N_y} \right) \left(1 - \frac{N}{N_z} \right) \left(\frac{1}{C_{bs,rem}} \right)^2 + \left(2 - \frac{N}{N_y} - \frac{N}{N_z} \right) \frac{N}{N_y} \frac{\pi^2 c \delta s}{C_{bs,rem1}} + \frac{3}{4} \left(\frac{N}{N_y} \right)^2 \left(\pi^2 c \delta s \right)^2 \right] + \left(\frac{M_{y,a,max}}{M_{y,max}} \right)^2 \left[\left(1 - \frac{N}{N_y} \right) \left(1 - \frac{N}{N_z} \right) \left(\frac{1}{C_{ba,rem}} \right)^2 + \frac{\left(1 - \frac{N}{N_y} \right) \left(1 - \frac{N}{N_z} \right)}{\left(1 - \frac{N}{N_{ya}} \right) \left(1 - \frac{N}{N_{za}} \right)} \left(\left(2 - \frac{N}{N_{ya}} - \frac{N}{N_{za}} \right) \frac{N}{N_{ya}} \frac{\pi^2 c \delta a}{C_{ba,rem1}} + \frac{1}{2} \left(\frac{N}{N_{ya}} \right)^2 \left(\pi^2 c \delta a \right)^2 \right] \right\}^{-0.5}$
$M_z = M_z^I$ Upper bound*)	M_y^I	M_z^I	$\sqrt{\frac{\zeta}{k_1}} \left[\left(\frac{M_{y,s,max}}{M_{y,max}} \frac{1}{C_{bs,rem}} \right)^2 + \left(\frac{M_{y,a,max}}{M_{y,max}} \frac{1}{C_{ba,rem}} \right)^2 \right]^{-0.5}$

*) The upper bound solution of $\frac{M_{y,max}}{M_{cr,0}}$ with the limiting condition $\frac{N}{N_{cr}} \leq 1$ where $N_{cr} = \min(N_y, N_z, N_T)$

In order to illustrate the analytical model solutions of present study for considered loading cases, the bisymmetric wide flange double-tee section is adopted, the properties of which are given in Table 3 (the section adopted is equivalent to a hot-rolled HEB 300 but consists of flange and web rectangle shape plates).

A proposal based on LBA and based on the decomposition of unequal end moments into symmetric and antisymmetric components was developed by Cuk and Trahair [5]. The solution was later presented in the form dependent upon the equivalent uniform moment

Table 2. Comparison of the equivalent uniform moment factors for QEA and LEA formulations in which the minor axis moment is that of the first order

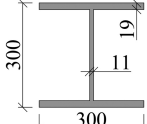
Type of analysis	Curvature v''_0	Moment M_z	Equivalent uniform moment factor C_{bc}
QEA	$-\frac{M_y^I + Nv_0}{EI_z}$	$M_z^I = M_y^I \phi$	$\sqrt{\xi} \left\{ \left(\frac{M_{y,s,\max}}{M_{y,\max}} \right)^2 \left[\left(1 - \frac{N}{N_z} \right) \left(\frac{1}{C_{bs,\text{rem}}} \right)^2 + \left(\frac{N}{N_z} \frac{1}{C_{bs,\text{cem}}} \right)^2 \right] + \left(\frac{M_{y,a,\max}}{M_{y,\max}} \right)^2 \left[\left(1 - \frac{N}{N_z} \right) \left(\frac{1}{C_{ba,\text{rem}}} \right)^2 + \frac{1 - \frac{N}{N_z}}{1 - \frac{N}{N_{za}}} \left(\frac{N}{N_{za}} \frac{1}{C_{ba,\text{cem}}} \right)^2 \right] \right\}^{-0.5}$
Upper bound*)	$-\frac{M_y^I}{EI_z}$	$M_z^I = 0$	$\sqrt{\xi} \left[\left(\frac{M_{y,s,\max}}{M_{y,\max}} \frac{1}{C_{bs,\text{rem}}} \right)^2 + \left(\frac{M_{y,a,\max}}{M_{y,\max}} \frac{1}{C_{ba,\text{rem}}} \right)^2 \right]^{-0.5}$
LEA**)	v''_0	$M_z = 0$	$\sqrt{\xi} \left[\left(\frac{M_{y,s,\max}}{M_{y,\max}} \frac{1}{C_{bs,\text{cem}}} \right)^2 + \frac{1 - \frac{N}{N_z}}{1 - \frac{N}{N_{za}}} \left(\frac{M_{y,a,\max}}{M_{y,\max}} \frac{1}{C_{ba,\text{cem}}} \right)^2 \right]^{-0.5}$

*) The upper bound solution of $M_{y,\max}/M_{cr,0}$ with the limiting condition $\frac{N}{N_{cr,op}} \leq 1$,

where $N_{cr,op} = \min(N_z, N_T)$

***) In conjunction with in-plane equilibrium set in the undeflected configuration, i.e. the amplification factor $1 / \left(1 - \frac{N}{N_y} \right) = 1$.

Table 3. Section properties of the equivalent section used in numerical models

	A	I_y	I_z	I_T	I_w	$W_{y,p1}$	$W_{z,p1}$	k_1
	mm ²	mm ⁴			mm ⁶	mm ³	mm ³	–
	142.8 × 10 ²	24187 × 10 ⁴	8553 × 10 ⁴	145 × 10 ⁴	1688 × 10 ⁹	1790 × 10 ³	863 × 10 ³	0.646

factor C_{bc} by Trahair et al. [16]. Such a proposal may be extended for any combined load case and written down as follows:

$$(2.2) \quad \frac{1}{C_{bc}} = \frac{M_{y,s,\max}}{M_{y,\max}} \frac{1}{C_{bs}} + \left(\frac{M_{y,a,\max}}{M_{y,\max}} \right)^3 \frac{1}{C_{ba}} \left(1 - 0.575 \frac{N}{N_z} \right)$$

where: C_{bs} – equivalent uniform symmetric moment component factor (equal to unity for equal and opposite moments, refer to Fig. 1a), C_{ba} – equivalent uniform antisymmetric moment component factor (approximated by taking 2.5 for equal end moments of the same direction, refer to Fig. 1b); the other symbols are the same as in the companion paper [7].

For the purpose of comparison with other solutions, the numerical values of C_{bs} and C_{ba} factors in Eq. (2.2) may be taken as those used in the Timoshenko Energy Method [14, 15], cf. Barszcz et al. [3], and confirmed by a general derivation presented in Barszcz et al. [2] for the elastic lateral-torsional buckling of beams.

Figure 3 shows the $M_{y,\max}/M_{cr,0} = C_{bc}\sqrt{F(N)}$ factors for the left end moment load case presented in Fig. 1a, from the analytical solutions summarized in Table 1, together with $F(N) = F_3(N)$ and $N/N_y = (1 - k_1)(N/N_z)$, and in Table 2, together with $F(N) = F_2(N)$. The section properties are given in Table 3. The analytical solutions are compared with that of Eq. (2.2) with C_{bs} and C_{ba} factors as given in Cuk and Trahair [5] and with the solution presented by Bijak [4].

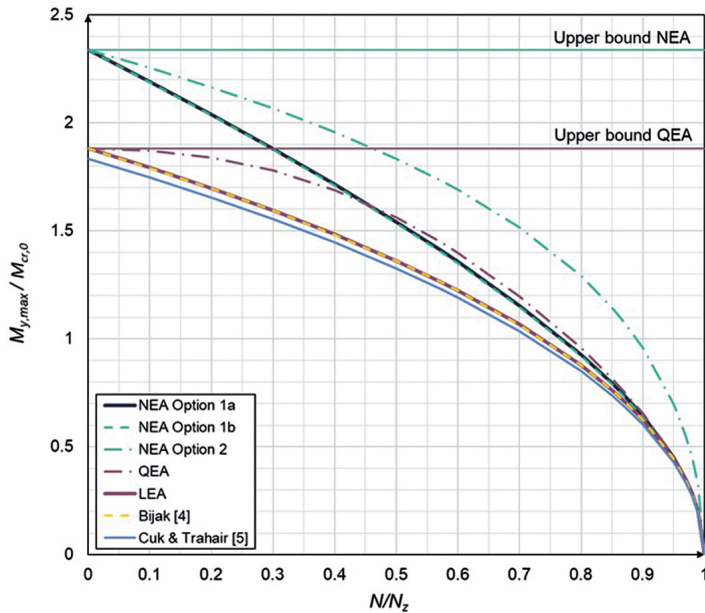


Fig. 3. Comparison of factor $M_{y,\max}/M_{cr,0}$ for the left end moment load case and $\lambda_{LT} = 1, 6$

Figure 4 shows the $M_{y,\max}/M_{cr,0}$ factors, from the analytical solutions summarized in Table 1 and Table 2, for the left half-length uniformly distributed load case presented in Fig. 1b. The analytical solutions are compared with that of Bijak [4], being equivalent to Eq. (2.15) of a companion paper [7] in which N/N_z and N/N_{za} are linear multipliers to the reciprocals of elementary conversion factors squared, and that of Trahair et al. [16], in the form of Eq. (2.2) in which $C_{bs} = C_{bs,\text{rem}}$, $C_{ba} = C_{ba,\text{rem}}$ of the present study are used.

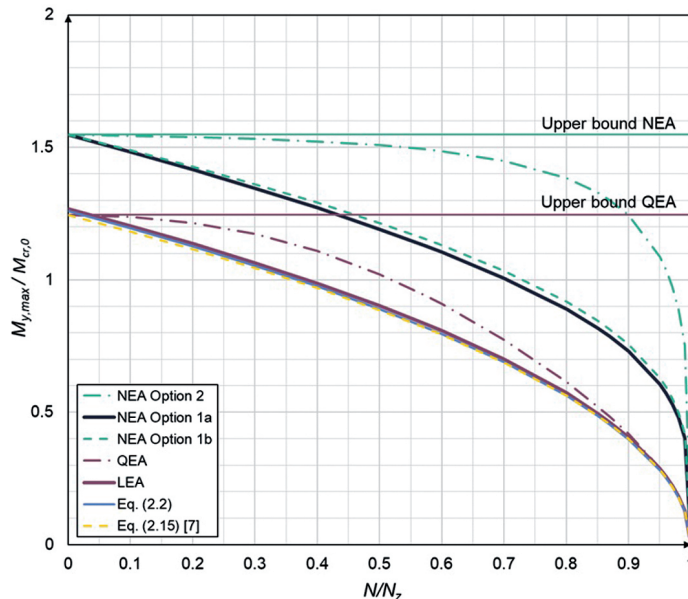


Fig. 4. Comparison of factor $M_{y,\max}/M_{cr,0}$ for the left half-length uniformly distributed load case and $\bar{\lambda}_{LT} = 2.0$

General observations from the comparison of analytical solutions are as follows:

1. Stability limit curves $M_{y,\max}/M_{cr,0}$ based on the classical solutions (LEA, Cuk and Trahair [3] and Trahair et al. [12]) are almost identical. The QEA solution is well above those based on the classical energy LEA method. The differences between the QEA solution and the other classical ones considered herein are dependent upon the slenderness ratio. For smaller slenderness ratio values, the QEA solution gives lower values of $M_{y,\max}/M_{cr,0}$ (except the extreme situation of $N/N_z = 1$ where all the solutions coincide).
2. In the range of the moment effect dominating over that of the effect of compressive force, the LEA curves are placed well below those based on NEA. On the other hand, in the range of the compressive force effect dominating over that of the moment one, the tendency is such that all the results are closer to each other for LTU beam-columns and coinciding at the point of $N_{cr,op} = \min(N_z, N_T) \ll N_y$.
3. NEA solutions of $M_{y,\max}/M_{cr,0}$ of present study, are placed well above those of classical solutions. This confirms the observation well known from the subject literature, e.g. Trahair [15] and Trahair et al. [16], that there is a great influence of the prebuckling deformation state on the lateral-torsional critical state and therefore also on the interaction between the instability modes in relation to compression alone and to major axis bending alone.
4. NEA Option 1a solution, that for symmetric loading patterns coincides with that of Mohri et al. [12], may be used for engineering practice since: a) it includes prebuck-

ling modes of failure, b) it requires the evaluation of less moment integral factors than that of the Option 1b, c) it results in the lower predictions of $M_{y,\max}/M_{cr,0}$ than the other NEA solutions. Such a solution is then recommended for the verification exercise and for comparison with numerical finite element results for asymmetric loading cases presented in the following section of this paper.

5. Finally, one has to bear in mind that the classical energy formulation coefficients $C_{bs,cm}$, $C_{ba,cm}$ used in LEA may lead to unsafe results of LTB for combined load cases in which end moments are acting together with span loads, cf. Barszcz et al. [2]. Figs. 3 and 4 proved that the NEA Option 1a solution of present study and using coefficients $C_{bs,rem}$, $C_{ba,rem}$ leads to more accurate predictions.

In the following, the analytical solution of NEA Option 1a from Table 1 is verified with use of results from numerical simulations. Numerical simulations are obtained with use of two worldwide recognized codes, namely Abaqus [1] and LTBeamN [11].

The line modeling technique conforming the Vlasov theory and using 7 degrees of freedom per node is adopted in the LTBeamN software.

The shell model of S4R, adopted in the Abaqus software, with a size of approximately 30 mm by 30 mm for flanges and the web of considered double-tee section is used. The boundary conditions for end sections are modelled using rigid sub-contours for two flanges and one sub-contour for the web with shell elements multipoint constrained as shown in Giżejowski et al. [10], cf. Fig. 5. Boundary conditions conform with the Vlasov theory of thin-walled sections so that the results from analytical models and from computer codes LTBeamN and Abaqus could be directly compared.

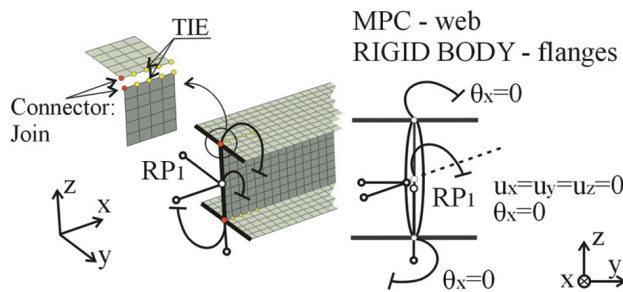


Fig. 5. Modelling of end section boundary conditions

Firstly, numerical simulations based on Linear Buckling Analysis (LBA) in the form of Linear Eigenproblem Analysis (LEA) are carried out by assuming the elastic behaviour in both LTBeamN and Abaqus codes for the ideally straight and residual stress free member. Next, numerical simulations based on Nonlinear Buckling Analysis (NBA) are carried out, using enhanced large displacement Geometrically and Materially Nonlinear Analysis (GMNA+) and Abaqus code for a quasi-perfect member geometry, residual stress free. The initial geometry assumed is that corresponding to the lowest LEA out-of-plane overall elastic instability mode with the amplitude scaled from unity to such a very small percentage of unity that ensures the numerical convergence. The material model in NBA is assumed to

be a bilinear elastic-plastic, with a very small isotropic hardening ratio of $E/10000$ in the inelastic region in order to avoid an early termination of GMNA+ type of numerical simulations. The results obtained with use of NBA for the quasi-ideal member geometry and a very small out-of-straightness amplitude ensuring the numerical convergence would indicate the failure mode associated with the inelastic out-of-plane buckling of beam-columns under different proportion between the in-plane stress resultants in bending and compression.

LBA numerical and analytical models are based on the eigenproblem formulation that allows for the bifurcation points detection on the primary equilibrium path, therefore they are based on separating the prebuckling and postbuckling states. In the problem investigated herein, beam-columns are subjected to a second order bending in the plane of section greater moment of inertia up to the first bifurcation point on the primary equilibrium path (the critical state). The postbuckling neutral equilibrium is associated with the second order minor axis bending and non-uniform torsion. LBA models use the stress resultants obtained from the Linear Analysis (LA) or Geometrically Nonlinear Analysis (GNA) identifying the prebuckling equilibrium path. The assumption of small postbuckling displacements holds, with no interaction between prebuckling and postbuckling deformation states. The prebuckling in-plane stability effects on the out-of-plane buckling state may only be investigated using enhanced Geometrically Nonlinear Analysis GNA+ (elastic for quasi-perfect geometry of beam-columns) or GMNA+ (inelastic for quasi-perfect geometry of beam-columns). The latter analysis is more suitable since it may indicate the mode of failure and a nature of the inelastic resistance of very slender structural members. Such an analysis was carried out in Giżejowski et al. [10], proving that the inelastic LTU beam-columns under major axis bending fail due to large twist rotations when associated with zero or very small value of the compressive force. The inelastic buckling resistance of quasi-perfect beams is therefore a decreasing function for the increasing member length. The beam buckling resistance approaches the section major axis bending resistance for stocky elements while the section minor axis bending resistance for very slender beams. When the compressive force increases over the major axis bending moment, the mode of failure becomes less associated with large twist rotations and it is related more to large values of the out-of-plane translations. When the compressive force is associated with a very small major axis maximum moment, the failure mode of a stocky column of the quasi-perfect geometry is due to yielding of all sections along the member length while for a slender column it is due to large quasi-elastic out-of-plane translations under the compressive force approaching the critical value.

The results obtained in Barszcz et al. [2] deal with the lateral-torsional buckling of beams under bending about the section stronger principal axis. The results based on the analytical formulation presented in [2] for beams are also shown hereafter just to indicate that the NEA Option 1 solution for beam-columns and for $N = 0$ coincides with that for beams.

In order to assess the failure mode and the resistance of a quasi-perfect geometry beam-column, numerical simulations are carried out for a very slender member being under the asymmetric load shown in Fig. 2a, the lateral-torsional slenderness $\bar{\lambda}_{LT}$ of which, corresponding to the lowest buckling mode is equal to approximately 2.0. The comparison of analytical results based on the following models: LEA, Trahair's approximation through

Eq. (2.2) and NEA Option 1a formulation of present study, and numerical results available from computer simulations using Abaqus and LTBeamN codes is shown in Fig. 6. Slender beam-columns, unrestrained laterally and torsionally, are sensitive to the out-of-plane modes of buckling much more than to the in-plane buckling modes. Because there is a weak interaction between in-plane and out-of-plane buckling modes, a substantial inelastic postbuckling reserve may exist in the buckling resistance evaluation of slender beam-columns. Such a reserve is expected to be negligible for low values of the maximum bending moment and for the compressive force approaching its critical value, associated with the lateral buckling mode. Contrarily, when the bending moment rises and the compressive force decreases, the lateral-torsional buckling mode starts to play an important role and the inelastic postbuckling reserve is expected to be more and more visible. In order to prove the above mentioned phenomenon, it is rational to carry out NBA in the form of GMNA+.

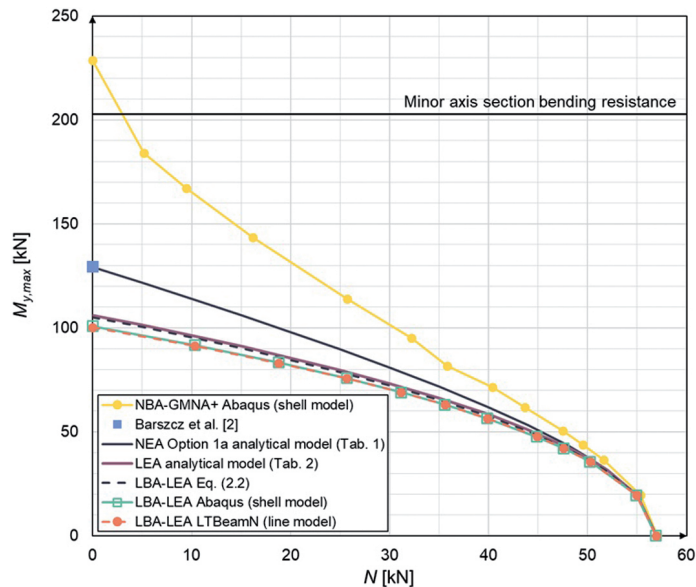


Fig. 6. Analytical and numerical $M_{y,max} - N$ flexural-torsional buckling limit curves for the half-length uniformly distributed load case

General observations from the comparison of analytical and numerical results of the considered LTU beam-columns are as follows:

1. The results from the analytical LBA LEA model of Table 2 are close to those from LBA numerical simulations of both LTBeamN and Abaqus. This confirms conclusions from the authors' earlier investigations that analytical flexural-torsional stability solutions based on the stress resultants from LA, and neglecting the effect of prebuckling displacements, describe accurately the numerical LBA results of elastic out-of-plane buckling, regardless the type of finite elements used.
2. Results based on a generalization of the formula proposed by Trahair et al. [16] agree quite well with those of LEA in Table 2.

3. Results from the LBA analytical model based on NEA Option 1a are placed higher than those discussed in 1. and 2. above. The differences are decreasing with the increase of the axial compressive force. All the discussed models give the same value equal to the out-of-plane critical force $N_{cr,op} = \min(N_z, N_T) = N_z$ for the major axis bending moment being equal to zero.
4. Figure 6 indicates that for very slender members without discrete LT restraints, the LBA numerical results obtained from both computer codes considered, represented in Fig. 6 by a set of discrete points are practically of the same lower bound curve. NBA GMNA+ finite element results, corresponding to the ultimate load of a quasi-straight geometry of the inelastic member, constitute the upper bound. The buckling resistance curve created by discrete points from the simulation results of GMNA+ exceeds the analytical elastic buckling curves, especially for lower values of the axial compressive force. For the compressive force equal to zero, the GMNA+ buckling resistance is well above the analytical elastic lateral-torsional buckling moment, that is the LEA elastic critical moment $M_{cr} = 106$ kN and NEA Option 1a ultimate moment $M_{cr}/\sqrt{k_1} = 129$ kN, and even slightly overestimates the section plastic resistance in minor axis bending $M_{z,pl} = 203$ kN·m.
5. The inelastic failure mode associated with the quasi-perfect geometry is associated with a very large twist rotation of about 90° attained at the ultimate state of the beam inelastic response. Such an effect was observed by Giżejowski et al. in [10] when studying the behaviour of quasi-straight beam-columns under moment gradient. A very large twist rotation is associated with a very large normal strain produced at the ultimate state by the minor axis bending and torsion, the strain that is well advanced in the hardening region. This in turn might give the ultimate state bending moment value exceeding the plastic hinge capacity of $M_{z,pl} = 203$ kN·m, calculated as for the $\sigma - \varepsilon$ model of an elastic-ideally-plastic constitutive law.
6. It has to be underlined that one cannot directly compare elastic LBA results and inelastic GMNA+ results, the latter obtained for the member of practically perfect geometry. The only conclusion one may invoke is that the NEA Option 1a elastic buckling results are much closer to the ultimate inelastic response for low values of N than those from LEA based formulations.
7. NEA results of the Options 1a, as the compressive force progresses from its zero value to the critical value of N_z , coincide with those from numerical simulations of GMNA+. For very low values of the maximum bending moment, the numerical results exceed slightly the elastic critical force in compression. This results from the fact that the material model is bilinear with a very small hardening effect in the inelastic region, so that the ultimate limit state is reached in association of the large plastic strain of section fibres.
8. Results from the LBA analytical model based on NEA Option 1a are closer to those from GMNA+ than those from all the other LBA analytical models. The differences decrease when the axial compressive force increases. Analytical LBA model based on NEA Option 1a appeared to be the most robust solution, therefore is recommended for practical applications.

3. Verification of recommended analytical solution for LTR beam-columns

3.1. Analytical solution for beam-columns with intermediate LT restraints

The analytical solutions presented in the companion paper of this study [7] may not be directly applicable in the Salvadori's method [13, 15, 16] for estimating the elastic stability limit curve of prismatic LTR beam-columns. The reason is that the symmetric and antisymmetric load components deal with the whole length $L_m = \sum_i L_i$ (where $i = 1, 2, \dots, r$ is the number of member segments of length L_i created by restraints, in this investigation spaced equally along the member length, so that $\sum_i L_i = rL$ and $L_i = L$) and not with the member segment. Hence, the second order moment components $M_{y,s}^{II}$ and $M_{y,a}^{II}$ for the whole member may give a complex combination of symmetric and antisymmetric moment components for member segments. In order to facilitate the solution of stability problems for discretely restrained (LTR) beam-columns, the complex moment diagram for the segment "i" must be decomposed into two components, i.e.:

- $M_{y,s,i}$ resulting from the symmetric load on the beam-column and associated with the in-plane lowest flexural mode of buckling that in turn may be divided into j -components of elementary symmetric components $M_{y,ss,i,j}$ and k -components of elementary antisymmetric components $M_{y,sa,i,k}$,
- $M_{y,a,i}$ resulting from the antisymmetric load on the beam-column and associated with the in-plane second lowest flexural mode of buckling that in turn may be divided into m -components of elementary antisymmetric components $M_{y,aa,i,m}$ and n -components of elementary symmetric components $M_{y,as,i,n}$.

As a result, the second order in-plane moment for the segment "i" becomes:

$$M_{y,i}^{II} = \frac{\sum_j M_{y,ss,i,j} + \sum_k M_{y,sa,i,k}}{1 - \frac{N}{N_y}} + \frac{\sum_m M_{y,aa,i,m} + \sum_n M_{y,as,i,n}}{1 - \frac{N}{N_{ya}}}$$

and the out-of-plane moment for the segment "i" stands for:

$$M_{z,i}^{II} = \frac{\left(\sum_j M_{y,ss,i,j} + \sum_n M_{y,as,i,n} \right) \phi_x}{1 - \frac{N}{N_{z,i}}} + \frac{\left(\sum_m M_{y,aa,i,m} + \sum_k M_{y,sa,i,k} \right) \phi_x}{1 - \frac{N}{N_{za,i}}}$$

Hence, the moment term in Eq. (2.18a) presented in the companion paper [7], and used for the NEA Option 1a of the segment “*i*” of the LTR beam-column, yields

$$\begin{aligned}
 & \frac{1}{2} \frac{k_1 L_i}{EI_z} \int_0^1 \delta \left\{ \left(\frac{\sum_j M_{y,ss,i,j} + \sum_k M_{y,sa,i,k}}{1 - \frac{N}{N_y}} + \frac{\sum_m M_{y,aa,i,m} + \sum_n M_{y,as,i,n}}{1 - \frac{N}{N_{ya}}} \right) \right. \\
 & \left. \phi_x \left[\frac{\left(\sum_j M_{y,ss,i,j} + \sum_n M_{y,as,i,n} \right) \phi_x}{1 - \frac{N}{N_{z,i}}} + \frac{\left(\sum_m M_{y,aa,i,m} + \sum_k M_{y,sa,i,k} \right) \phi_x}{1 - \frac{N}{N_{za,i}}} \right] \right\} d\xi \\
 & = \frac{k_1 L_i}{EI_z} \delta a_3 \int_0^1 \left\{ \frac{\sum_j M_{y,ss,i,j} \left(\sum_j M_{y,ss,i,j} + \sum_n M_{y,as,i,n} \right) \sin^2(\pi\xi)}{\left(1 - \frac{N}{N_y}\right) \left(1 - \frac{N}{N_{z,i}}\right)} \right. \\
 & + \frac{\sum_n M_{y,as,i,n} \left(\sum_j M_{y,ss,i,j} + \sum_m M_{y,as,i,m} \right) \sin^2(\pi\xi)}{\left(1 - \frac{N}{N_{ya}}\right) \left(1 - \frac{N}{N_{z,i}}\right)} \\
 & + \frac{\sum_k M_{y,sa,i,k} \left(\sum_m M_{y,aa,i,m} + \sum_k M_{y,sa,i,k} \right) \sin^2(\pi\xi)}{\left(1 - \frac{N}{N_y}\right) \left(1 - \frac{N}{N_{za,i}}\right)} \\
 & \left. + \frac{\sum_m M_{y,aa,i,m} \left(\sum_m M_{y,aa,i,m} + \sum_k M_{y,sa,i,k} \right) \sin^2(\pi\xi)}{\left(1 - \frac{N}{N_{ya}}\right) \left(1 - \frac{N}{N_{za,i}}\right)} \right\} d\xi
 \end{aligned}$$

The basic critical state relationship $M_{y,\max} - N$ given in [7], and adopted herein for the critical segment “*i*” as an approximation of the critical state of the prismatic beam-column with equally spaced LT restraints may be written down as:

$$(3.1) \quad \left(\frac{M_{y,i,\max}}{C_{bc,i} M_{cr,0,i}} \right)^2 = \left(1 - \frac{N}{N_y}\right) \left(1 - \frac{N}{N_{z,i}}\right) \left(1 - \frac{N}{N_{T,i}}\right)$$

where: $M_{y,i,\max}$ – maximum moment of the segment “*i*”, N_y – lowest in-plane flexural buckling force of the system, $N_{z,i}$ – lowest out-of-plane flexural buckling force of the critical segment, $N_{T,i}$ – lowest torsional buckling force of the critical segment, $M_{cr,0,i} =$

$i_0\sqrt{N_{z,i}N_{T,i}}$ – lateral-torsional critical moment of the critical segment under uniform bending.

The equivalent uniform moment conversion factor, evaluated in the presence of axial compression, takes of the following form:

$$(3.2) \quad \frac{1}{C_{bc,i}} = \sqrt{\frac{k_1}{\zeta}} \left[\left(\frac{M_{y,s,i,\max}}{M_{y,i,\max}} \right)^2 \left(\frac{1}{C_{bss,\text{rem},i}^2} + \frac{1 - \frac{N}{N_{z,i}}}{1 - \frac{N}{N_{za,i}}} \frac{1}{C_{bsa,\text{rem},i}^2} \right) \right. \\ \left. + \frac{M_{y,s,i,\max}M_{y,a,i,\max}}{M_{y,i,\max}^2} \left(1 + \frac{1 - \frac{N}{N_y}}{1 - \frac{N}{N_{ya}}} \right) \left(\frac{1}{C_{bss,as,\text{rem},i}^2} + \frac{1 - \frac{N}{N_z}}{1 - \frac{N}{N_{za,i}}} \frac{1}{C_{bsa,aa,\text{rem},i}^2} \right) \right. \\ \left. + \frac{1 - \frac{N}{N_y}}{1 - \frac{N}{N_{ya}}} \left(\frac{M_{y,a,i,\max}}{M_{y,i,\max}} \right)^2 \left(\frac{1}{C_{bas,\text{rem},i}^2} + \frac{1 - \frac{N}{N_{z,i}}}{1 - \frac{N}{N_{za,i}}} \frac{1}{C_{baa,\text{rem},i}^2} \right) \right]^{0.5}$$

where:

$$\frac{1}{C_{bss,\text{rem},i}^2} = 2 \int_0^1 \left(\frac{\sum_j M_{y,ss,i,j}}{M_{y,s,i,\max}} \right)^2 \sin^2(\pi\xi) d\xi$$

$$\frac{1}{C_{bsa,\text{rem},i}^2} = 2 \int_0^1 \left(\frac{\sum_k M_{y,sa,i,k}}{M_{y,s,i,\max}} \right)^2 \sin^2(\pi\xi) d\xi$$

$$\frac{1}{C_{bss,as,\text{rem},i}^2} = 2 \int_0^1 \frac{\sum_j M_{y,ss,i,j}}{M_{y,s,i,\max}} \frac{\sum_m M_{y,as,i,m}}{M_{y,a,i,\max}} \sin^2(\pi\xi) d\xi$$

$$\frac{1}{C_{bsa,aa,\text{rem},i}^2} = 2 \int_0^1 \frac{\sum_k M_{y,sa,i,k}}{M_{y,s,i,\max}} \frac{\sum_n M_{y,aa,i,n}}{M_{y,a,i,\max}} \sin^2(\pi\xi) d\xi$$

$$\frac{1}{C_{bas,\text{rem},i}^2} = 2 \int_0^1 \left(\frac{\sum_m M_{y,as,i,m}}{M_{y,a,i,\max}} \right)^2 \sin^2(\pi\xi) d\xi$$

$$\frac{1}{C_{baa,\text{rem},i}^2} = 2 \int_0^1 \left(\frac{\sum_n M_{y,aa,i,n}}{M_{y,a,i,\max}} \right)^2 \sin^2(\pi\xi) d\xi$$

and for $N = 0$ the following lower bound relationship is held:

$$\begin{aligned} \frac{1}{C_{bc,i}} = & \sqrt{\frac{k_1}{\zeta}} \left[\left(\frac{M_{y,s,i,\max}}{M_{y,i,\max}} \right)^2 \left(\frac{1}{C_{bss,\text{rem},i}^2} \right) + 2 \frac{M_{y,s,i,\max}}{M_{y,i,\max}} \frac{M_{y,a,i,\max}}{M_{y,i,\max}} \left(\frac{1}{C_{bss,as,\text{rem},i}^2} \right) \right. \\ & + \left. \left(\frac{M_{y,a,i,\max}}{M_{y,i,\max}} \right)^2 \left(\frac{1}{C_{bas,\text{rem},i}^2} \right) + \left(\frac{M_{y,s,i,\max}}{M_{y,i,\max}} \right)^2 \left(\frac{1}{C_{bsa,\text{rem},i}^2} \right) \right. \\ & \left. + 2 \frac{M_{y,s,i,\max}}{M_{y,i,\max}} \frac{M_{y,a,i,\max}}{M_{y,i,\max}} \left(\frac{1}{C_{bsa,aa,\text{rem},i}^2} \right) + \left(\frac{M_{y,a,i,\max}}{M_{y,i,\max}} \right)^2 \left(\frac{1}{C_{baa,\text{rem},i}^2} \right) \right]^{0.5} \end{aligned}$$

For an unrestrained beam of the length L (where $I = 1$ and $M_{y,i,\max} = M_{y,\max}$, $M_{y,s,i,\max} = M_{y,s,\max}$, $M_{y,a,i,\max} = M_{y,a,\max}$), being under one loading type (end moments, half-length uniformly distributed loads or one concentrated force in the half-length), no bending moments $\sum_k M_{y,sa,i,k}$ and $\sum_m M_{y,as,i,m}$ occur. Then, it is possible to convert the above relationship to that obtained for beams in [2]. For LT restrained beam-columns, Eq. (3.2) is concerned with the critical segment “ i ”, therefore creates a general lower bound solution. One must bear in mind that the critical segment “ i ” moment distribution, being a superposition of globally amplified symmetric and antisymmetric distributions, need to be decomposed into several elementary symmetric and antisymmetric components.

3.2. Case study of mid-length restrained beam-column under left end moment

Figure 7a shows the beam-column laterally and torsionally restrained in mid-length, together with the globally decomposed bending moments. The section and load case are those used for the unrestrained beam-column (Fig. 1a). Because of the LT restraint, the out-of-plane slenderness ratio $\bar{\lambda}_z$ of the restrained beam-column is reduced by 50% in comparison with that corresponding to its unrestrained counterpart, so that also the slenderness $\bar{\lambda}_{LT}$ is reduced. The failure mode of quasi-perfect geometry beam-columns is therefore controlled more by moderate lateral translations than by large twist rotations.

The identified critical segment is that between the left support and the mid-length LT restraint. Figure 7b shows the bending moment components of the critical segment needed for the evaluation equivalent uniform moment factor components. Table 4 summarizes the number of bending moment components for the critical segment and field moment equations. The equivalent uniform moment component factors corresponding to the field moment from Table 4 are listed in Table 5.

The analytical solution NEA Option 1a based on the Vlasov beam theory, presented in a companion paper and the previous subsection of this paper, is used hereafter with the factors given in Table 5 to obtain the approximate relationship between the axial compressive force and the maximum major axis bending moment at the critical state estimate of the considered LTR beam-column. The results are illustrated in Fig. 8 together with the verification of analytical results using computer finite element simulations. LBA

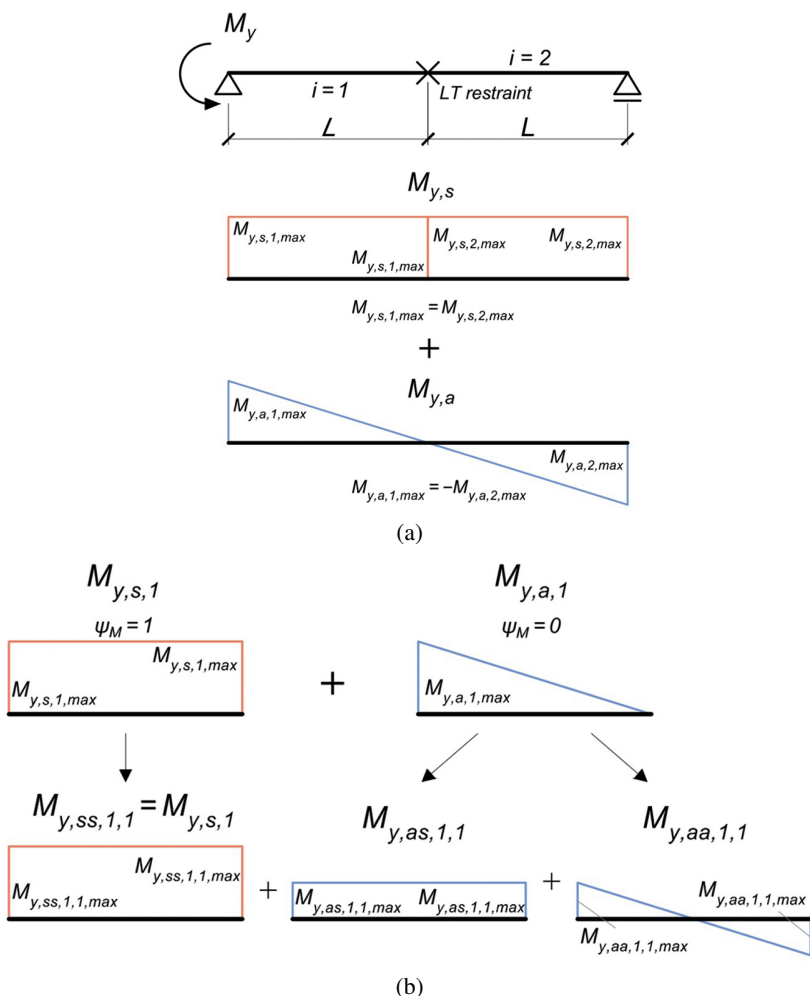


Fig. 7. Restrained beam-column with left end moment: a) static scheme and global symmetric and antisymmetric moment components for the in-plane amplification, b) bending moment decomposition for the critical segment

Table 4. Critical segment field moment equations

Load decomposition	Associated moment ratio	Field moment equations	
Symmetry $j = \{1\}, k = \{0\}$	$M_{y,s,1,max} = 0.5 M_{y,max}$	$M_{y,ss,1,1}$	$0.5 M_{y,max}$
		$M_{y,sa,1,0}$	0
Antisymmetry $n = \{1\}, m = \{1\}$	$M_{y,a,1,max} = 0.5 M_{y,i,max}$	$M_{y,as,1,1}$	$0.25 M_{y,max}$
		$M_{y,aa,1,1}$	$0.25 M_{y,max} \left(1 - \frac{2x}{L}\right)$

numerical models were built, of a shell type in Abaqus and a line (beam) type in LTBeamN. Such models are concerned with LEA. The third numerical model GMNA+ is the shell model with an initial crookedness corresponding to the lowest flexural-torsional mode and the amplitude as small as possible in order to ensure the convergence of incremental-iterative numerical solution of NBA in the numerical prediction of the full nonlinear path associated with the stable equilibrium.

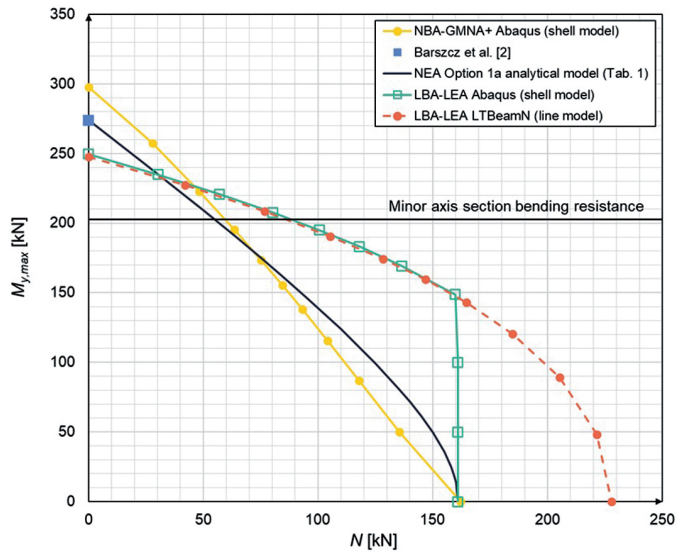


Fig. 8. Comparison of analytical and numerical $M_{y,max} - N$ flexural-torsional buckling limit curves for the load case of left support moment

Table 5. Equivalent uniform moment factor components

Symmetry		Antisymmetry		Others	
$\frac{1}{C_{bss,rem,i}^2}$	$\frac{1}{C_{bsa,rem,i}^2}$	$\frac{1}{c_{baa,rem,i}^2}$	$\frac{1}{c_{bas,rem,i}^2}$	$\frac{1}{c_{bss,as,rem,i}^2}$	$\frac{1}{c_{bsa,aa,rem,i}^2}$
1	0	0.0327	0.25	0.5	0

3.3. Case study of mid-length restrained beam-column under half-length uniformly distributed load

The second example of case study is concerned with the beam-column of the geometry and LT restraint being shown in Fig. 7 but with a different loading condition. The loading condition and the bending moment diagram are shown in Fig. 9a.

The identified critical segment is that between the left support and the mid-length LT restraint. Figure 9b shows the bending moment components needed for the evaluation of

equivalent uniform moment factor components. Table 6 summarizes the number of bending moment components for the critical segment and field moment equations. The equivalent uniform moment component factors corresponding to the field moment from Table 6 are listed in Table 7.

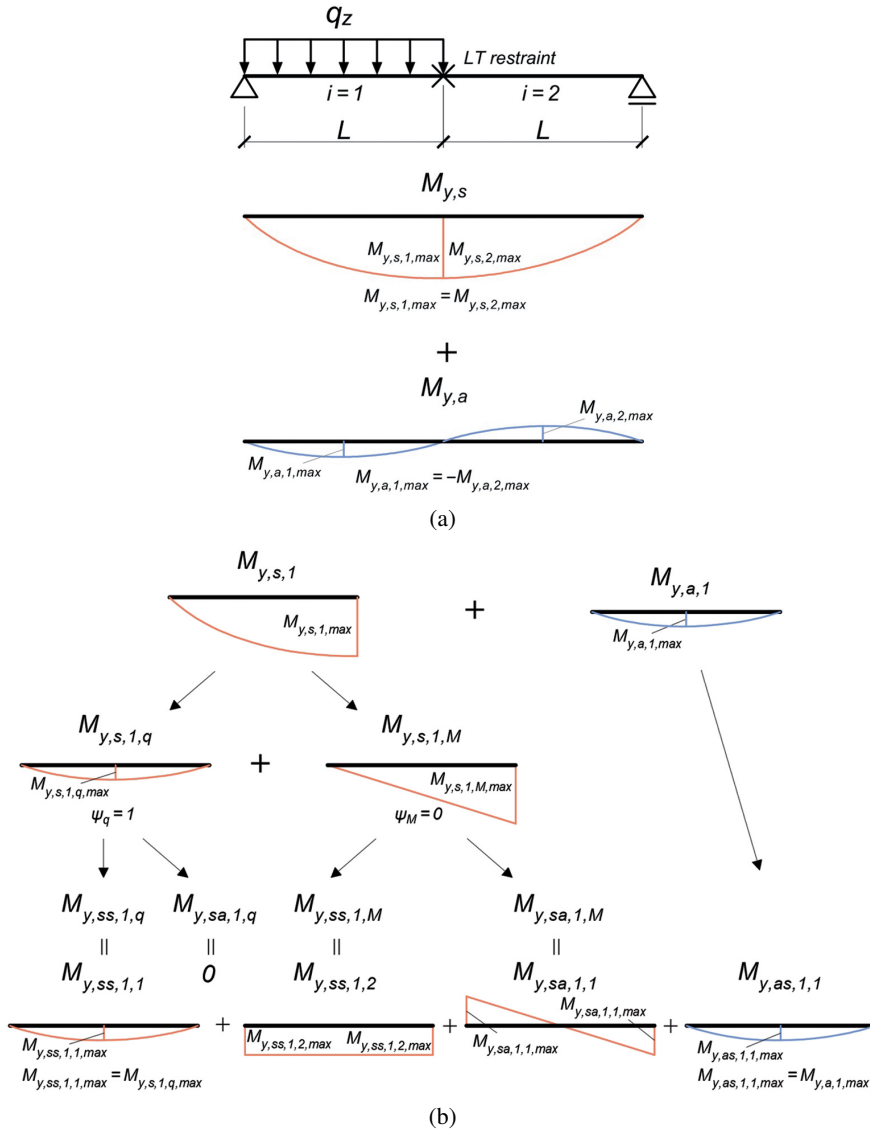


Fig. 9. Restrained beam-column with half-length uniformly distributed load: a) static scheme and global symmetric and antisymmetric moment components for the in-plane amplification, b) bending moment components for the critical segment (between the left support and the mod-length LT restraint)

Table 6. Critical segment field moment equations

Load decomposition	Associated moment ratio	Field moment equations	
Symmetry $j = \{1, 2\}, k = \{1\}$	$M_{y,s,1,max} = \frac{8}{9} M_{y,max}$	$M_{y_{ss},1,1}$	$\frac{8}{9} M_{y,max} \frac{x}{L} \left(1 - \frac{x}{L}\right)$
		$M_{y_{ss},1,2}$	$\frac{4}{9} M_{y,max}$
		$M_{y_{sa},1,1}$	$\frac{4}{9} M_{y,max} \left(1 - 2\frac{x}{L}\right)$
Antisymmetry $n = \{1\}, m = \{0\}$	$M_{y,a,1,max} = \frac{2}{9} M_{y,max}$	$M_{y_{as},1,1}$	$\frac{8}{9} M_{y,max} \frac{x}{L} \left(1 - \frac{x}{L}\right)$
		$M_{y_{aa},1,0}$	0

Table 7. Equivalent uniform moment factor components

Symmetry		Antisymmetry		Others	
1	1	1	1	1	1
$C_{bss,rem,i}^2$	$C_{bsa,rem,i}^2$	$c_{baa,rem,i}^2$	$c_{bas,rem,i}^2$	$c_{bss,as,rem,i}^2$	$c_{bsa,aa,rem,i}^2$
0.516	0.0327	0	0.780	0.630	0

The analytical solution NEA Option 1a is used again with the factors given in Table 7 to obtain the approximate relationship between the axial compressive force and the maximum major axis bending moment at the critical state of the considered LTR beam-column. The results are illustrated in Fig. 10 together with the verification of analytical results

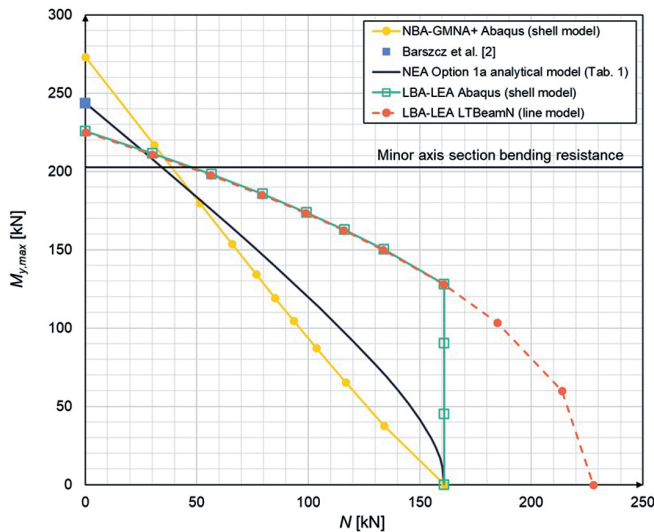


Fig. 10. Comparison of analytical and numerical $M_{y,max} - N$ flexural-torsional buckling limit curves for the half-length uniformly distributed load case

using computer finite element models. LBA numerical models was built, shell in Abaqus and line in LTBeamN. Such models are concerned with LEA. The third numerical model GMNA+ is the shell model with an initial crookedness corresponding to the lowest flexural-torsional mode and the amplitude as small as possible in order to ensure the convergence of incremental-iterative numerical solution for the nonlinear equilibrium path associated with the stable equilibrium. Comparison of results for the beam-column considered is shown in Fig. 10.

3.4. Summary of results from case study of FTB of restrained beam-columns

General observations from the comparison of analytical and numerical results of LTR beam-columns are as follows:

1. From the comparison of LBA LTBeamN and Abaqus numerical results it is obvious that Abaqus software can trace all the lowest buckling modes while LTBeamN only the out-of-plane buckling modes. The LTBeamN code predicts the results even for $N > N_y$, i.e. beyond the lowest buckling mode in pure compression, up to the bifurcation lowest out-of-plane force $N_z < N_T$ which is the second lowest buckling mode obtained from Abaqus simulations.
2. Numerical NBA results of GMNA+ for a quasi-straight geometry member are placed well below those corresponding to LBA, except for the range of small in-plane bending moment. It is very important noticing that LBA type of analysis carried out by Abaqus is not able to detect coupling between the in-plane and out-of-plane buckling modes. For the region of balanced values of compression and bending stress resultants, the LBA results overestimate the buckling resistance predicted by GMNA+. On the other hand, the buckling resistance estimated with use of GMNA+ is for $N = 0$ greater than the minor axis section bending resistance, much greater than that detected for the LTU beam-column (cf. Fig. 8). Since the lateral-torsional slenderness is in this case much lesser than that for the LTU beam-column, the buckling inelastic resistance of LTR beam-column is attained in this case for minor axis bending and compression of a laterally continuous static scheme. Only a moderate twist rotation of several degrees is achieved in the failure state, in contrast to that of 90° for the LTU beam-column ultimate limit state. The lateral displacements are however greater at failure than those for LTU beam-columns, due to the observed advancement of the plastic zones in section flanges.
3. The mid-section LT restraint acts as an internal support for the out-of-plane bending and torsion in simulations based on GMNA+, therefore, for the low compressive forces, it results in a moderate plastic zone spread, increasing the beam-column buckling resistance less importantly beyond that corresponding to the minor axis section resistance.
4. Results of the analytical solution of NEA Option 1a, based on the Salvadori's method for the critical segment, allows for a safe prediction by taking the coupling effect of in-plane and out-of-plane buckling modes into consideration.

5. NEA Option 1a solution developed in these investigations is recommended for practical application in the Eurocode's General Method (GM) of modern design procedures for both LTU and LTR elements of steelwork. Such a procedure has been presented in the earlier studies at the Warsaw University of Technology and presented in Gizejowski et al. [8, 9].

4. Summary and conclusions

The refined energy equation developed in Part I of this study [7] was summarized, then illustrated and verified for selected loading conditions by the results made available through numerical simulations for laterally and torsionally unrestrained (LTU) beam-columns. Theoretical investigations have been extended in Part II for beam-columns laterally and torsionally restrained (LTR). It has been proven that out-of-plane discrete rigid restraints have a great impact on the buckling state of beam-columns. One must bear in mind that the computer LBA simulations are based on the LEA formulation for the assessment of the elastic buckling stability of beam-columns, therefore are not able to account for coupling between in-plane and out-of-plane buckling modes (Abaqus software) or even cannot detect the in-plane modes (LTBeamN software). The approximate analytical solutions based on NEA have in this case an advantage over such numerical simulations.

The most suitable version of NEA analytical solution is that named herein as the Option 1a, therefore it has been recommended for practical application. This option of NEA has been shown to be especially vital for the analytical stability assessment of the flexural-torsional buckling of LTR beam-columns. The approximate analytical solution based on the NEA Option 1a and Salvadori's concept of the critical segment of LTR beam-columns was verified with use of numerical results from finite element simulations and proven to be a suitable lower bound estimation of the system buckling state. Detailed conclusions were presented in section 3 and 4 of Part II of this paper.

The analytical solutions developed in the paper include not only the effect of prebuckling stress resultants (axial force and major axis bending moment) on the elastic buckling state but also the effect of prebuckling deflections. The latter effect cannot be incorporated in the linear eigenproblem analysis (LEA) as implemented in computer codes dealt with. LEA results show that in-plane and out-of-plane buckling modes are treated as independent. In reality, all buckling modes suppose to be coupled. In order to prove that all the buckling modes are coupled, one may carry out GMNA+ (large displacement inelastic analysis), where "+" indicates a small disturbance of the perfect geometry taken into consideration in GMNA. This enables to predict the limit point on the static response equilibrium path and prove, or reject, the statement that global in-plane and out-of-plane buckling modes are coupled. The GMNA+ simulations carried out by authors proved that the buckling modes are strongly coupled for LTR beam-columns. One should not expect that the numerical results of GMNA+ would be comparable with those of the analytical solution for elastic members of perfect geometry. Numerical GMNA+ results of the maximum moment vs. the compressive force at the ultimate state constitute a "concave curve type" while those

corresponding to analytical results of the elastic bifurcation instability constitute a “convex curve type”. The only observation one may make is that both, numerical GMNA+ results and analytical results of the Option 1a solution prove that there is an unavoidable interaction between the in-plane and out-of-plane buckling modes.

The outcomes of presented paper are important for a further development of the Eurocode 3 General Method (GM) that is a modern design method for the overall buckling resistance check, developed for multiple stress resultant stability problems, dedicated to compression and major axis bending of open section members.

Acknowledgements

This paper presents a continuation of research undertaken in [13] where the theoretical basis has been developed. The solutions obtained in the companion Part I of this paper were verified for selected asymmetric loading cases using the results of numerical simulations of the flexural-torsional buckling of beam-columns. Both LTU and LTR beam-columns are dealt with. Authors write the paper in the memory of late Professor Nicholas Snowden Trahair of the University of Sydney and with thank to his constant encouragement in research on the space instability of steel structures. The first author of this paper carried out the postdoctoral study under his leadership in 80s of the last century.

References

- [1] Abaqus/Standard User's manual, Version 6.11. Dassault Systèmes, 2011.
- [2] A.M. Barszcz, M.A. Giżejowski, and M. Pękacka, “Elastic lateral-torsional buckling of steel bisymmetric double-tee section beams”, *Archives of Civil Engineering*, vol. 68, no. 2, pp. 83–103, 2022, doi: [10.24425/ace.2022.140631](https://doi.org/10.24425/ace.2022.140631).
- [3] A.M. Barszcz, M.A. Giżejowski, and Z. Stachura, “On elastic lateral-torsional buckling analysis of simply supported I-shape beams using Timoshenko's energy method”, in *Modern trends in research on steel, aluminium and composite structures*, M. Giżejowski, et al., Eds. London: Routledge, 2021, pp. 92–98, ISBN 9781003132134.
- [4] R. Bijak, “Lateral-torsional buckling of simply supported bisymmetric beam-columns”, *Journal of Civil Engineering, Environment and Architecture*, vol. 64, no. 3, pp. 461–470, 2017 (in Polish), doi: [10.7862/rb.2017.138](https://doi.org/10.7862/rb.2017.138).
- [5] P.E. Cuk and N.S. Trahair, “Elastic buckling of beam-columns with unequal end moments”, *Civil Engineering Transactions, Institution of Engineers, Australia*, 1981, vol. 3, pp. 166–171.
- [6] M. Giżejowski, A.M. Barszcz, and J. Uziak, “Elastic buckling of thin-walled beam-columns based on a refined energy formulation”, in *Modern trends in research on steel*, M. A. Giżejowski, et al., Eds. London: Routledge, Taylor & Francis Group, 2021, pp. 171–177.
- [7] M. Giżejowski, A.M. Barszcz, and P. Wiedro, “Refined energy formulation for the elastic flexural-torsional buckling of steel H-section beam-columns. Part I: Formulation and solutions”, *Archives of Civil Engineering*, vol. 69, no. 1, 2023 (submitted).
- [8] M.A. Gizejowski, Z. Stachura, R.B. Szczerba, and M.D. Gajewski, “Buckling resistance of steel H-section beam-columns: In-plane buckling resistance”, *Journal of Constructional Steel Research*, vol. 157, pp. 347–358, 2019, doi: [10.1016/j.jcsr.2019.03.002](https://doi.org/10.1016/j.jcsr.2019.03.002).
- [9] M.A. Gizejowski, Z. Stachura, R.B. Szczerba, and M.D. Gajewski, “Out-of-plane buckling resistance of rolled steel H-section beam-columns under unequal end moments”, *Journal of Constructional Steel Research*, vol. 160, pp. 153–168, 2019, doi: [10.1016/j.jcsr.2019.05.016](https://doi.org/10.1016/j.jcsr.2019.05.016).

- [10] M.A. Giżejowski, R. Szczerba, Z. Stachura, and M.D. Gajewski, “Buckling resistance of quasi-straight H-section beam-columns under unequal end moments”, *Archives of Civil Engineering*, vol. 67, no. 1, pp. 323–348, 2021, doi: [10.24425/ace.2021.136476](https://doi.org/10.24425/ace.2021.136476).
- [11] LTBeamN software version 1.0.3. Lateral Torsional Buckling, CTICM.
- [12] F. Mohri, Ch. Bouzerira, and M. Potier-Ferry, “Lateral buckling of thin-walled beam-column elements under combined axial and bending loads”, *Thin-Walled Structures*, vol. 46, no. 3, pp. 290–302, 2008, doi: [10.1016/j.tws.2007.07.017](https://doi.org/10.1016/j.tws.2007.07.017).
- [13] M.G. Salvadori, “Lateral torsional buckling of beams of rectangular cross-section under bending and shear”, in *Proceedings First US National Congress of Applied Mechanics*. 1951, pp. 403–405.
- [14] S.P. Timoshenko and J.M. Gere, *Theory of Elastic Stability*, 2nd ed. New York: McGraw-Hill, 1961.
- [15] N.S. Trahair, *Flexural-Torsional Buckling of Structures*. Boca Raton: CRC Press, 1993.
- [16] N.S. Trahair, M.A. Bradford, D.A. Nethercot, and L. Gardner, *The behaviour and design of steel structures to EC3*. 2nd ed. London-New York: Taylor and Francis, 2008.

Udoskonalona metoda energetyczna sprężystego wyboczenia giętno-skrętnego stalowych elementów ściskanych i zginanych o przekroju dwuteowym

Słowa kluczowe: stalowy element ściskany i zginany, dwuteownik bisymetryczny, zachowanie sprężyste, wyboczenie giętno-skrętne, symulacje numeryczne, weryfikacja rozwiązań analitycznych

Streszczenie:

W I części niniejszej pracy zastosowano różne rodzaje aproksymacji w analizie wyboczenia giętno-skrętnego elementów ściskanych i zginanych w płaszczyźnie większej bezwładności przekroju. Punktem wyjścia było sformułowanie zależności na pole przemieszczeń w konfiguracji odkształconej. Pokazano, że macierz rotacji, otrzymana przy zachowaniu funkcji trygonometrycznych średniego kąta skręcenia, jest wystarczająco dokładna do analizy stateczności giętno-skrętnej. Szczególną uwagę zwrócono w Części I na sformułowanie ogólnego równania energetycznego dla FTB, wyrażonego w funkcji siłprzekrojowych na podstawowej ścieżce równowagi, przed utratą płaskiej postaci zginania II rzędu, a także wpływu efektu ugięć w płaszczyźnie większej bezwładności przekroju, wyrażonego za pomocą współczynnika k_1 . Otrzymane równanie energetyczne zostało przedstawione w kilku wariantach zależnych od założeń upraszczających, jakie można przyjąć do rozwiązywania problemów wyboczenia giętno-skrętnego, tj. w postaci klasycznej analizy liniowego problemu własnego (LEA), w postaci kwadratowego problemu własnego (QEA) oraz w postaci udoskonalonej (nieklasycznej) analizy nieliniowego problemu własnego (NEA). W części II, w pierwszej kolejności, została zbadana i dyskutowana dokładność otrzymanych rozwiązań analitycznych w odniesieniu do propozycji przedstawionych we wcześniejszych opracowaniach. Przeprowadzone są też porównania dla rozwiązań w postaci zamkniętej uzyskanych w Części I, z oceną rozrzutu wyników, po przyjęciu $k_1 = 1$ w rozwiązaniach odpowiadających LEA i QEA, a także wszystkich opcji w rozwiązaniach odpowiadających NEA. Do dalszych badań rekomendowano najbardziej wiarygodne rozwiązanie analityczne. Szczegółowej weryfikacji poddano rozwiązania uzyskane dla wybranych asymetrycznych przypadków obciążenia: momentem na lewej podporze i równomiernie rozłożonym obciążeniem w połowie długości nieusztwionego, smukłego elementu ściskanego i zginanego. Ponadto w Części II zbadano, w jaki sposób kryterium wyboczeniowe, uzyskane dla elementu ściskanego

i zginanego bez usztywnień poprzecznych i przeciwskrętnych między przekrojami końcowymi, może być zastosowane dla elementu z dyskretnymi stężeniami poprzecznymi. Zalecane rozwiązania analityczne zweryfikowano z wykorzystaniem wyników numerycznych metody elementów skończonych dla elementów stężonych w przekroju środkowym. Wariant analitycznej postaci rozwiązania zalecanego w zaprezentowanych badaniach może być wykorzystany w praktyce w eurokodowej Metodzie Ogólnej (GM).

Received: 2022-09-02, Revised: 2022-12-13